THE JOURNAL OF BIOLOGICAL CHEMISTRY VOL. 284, NO. 43, pp. 29470–29479, October 23, 2009
Printed in the U.S.A.

Deletion of the Chloride Transporter Slc26a7 Causes Distal Renal Tubular Acidosis and Impairs Gastric Acid Secretion*[S]

Received for publication, July 15, 2009, and in revised form, August 18, 2009 Published, JBC Papers in Press, September 1, 2009, DOI 10.1074/jbc.M109.044396

Jie Xu[‡§], Penghong Song[¶], Suguru Nakamura[‖], Marian Miller[**], Sharon Barone[§‡‡], Seth L. Alper[§§], Brigitte Riederer[¶], Janina Bonhagen[¶], Lois J. Arend[¶¶], Hassane Amlal[§‡‡], Ursula Seidler[¶], and Manoocher Soleimani[‡§‡‡1]

From [‡]Research Services, Veterans Affairs Medical Center, Cincinnati, Ohio 45220 the [§]Department of Medicine, University of Cincinnati, Cincinnati, Ohio 45267, the [¶]Department of Gastroenterology, University of Hannover, 30625 Hannover, Germany, the [‖]Department of Biological Sciences, Murray State University, Murray, Kentucky 42071, the Departments of [**]Environmental Health and [¶¶]Pathology, University of Cincinnati, Cincinnati, Ohio 45267, the [§§]Renal Division, Beth Israel Deaconess Medical Center, and Department of Medicine, Harvard Medical School, Boston, Massachusetts 02115, and the [‡‡]Center on Genetics of Transport and Epithelial Biology, University of Cincinnati, Cincinnati, Ohio 45267

SLC26A7 (human)/Slc26a7 (mouse) is a recently identified chloride-base exchanger and/or chloride transporter that is expressed on the basolateral membrane of acid-secreting cells in the renal outer medullary collecting duct (OMCD) and in gastric parietal cells. Here, we show that mice with genetic deletion of Slc26a7 expression develop distal renal tubular acidosis, as manifested by metabolic acidosis and alkaline urine pH. In the kidney, basolateral Cl^-/HCO_3^- exchange activity in acid-secreting intercalated cells in the OMCD was significantly decreased in hypertonic medium (a normal milieu for the medulla) but was reduced only mildly in isotonic medium. Changing from a hypertonic to isotonic medium (relative hypotonicity) decreased the membrane abundance of Slc26a7 in kidney cells *in vivo* and *in vitro*. In the stomach, stimulated acid secretion was significantly impaired in isolated gastric mucosa and in the intact organ. We propose that SLC26A7 dysfunction should be investigated as a potential cause of unexplained distal renal tubular acidosis or decreased gastric acid secretion in humans.

The collecting duct segment of the distal kidney nephron plays a major role in systemic acid base homeostasis by acid secretion and bicarbonate absorption. The acid secretion occurs via H^+-ATPase and H-K-ATPase into the lumen and bicarbonate is absorbed via basolateral Cl^-/HCO_3^- exchangers (1–4). The tubules, which are located within the outer medullary region of the kidney collecting duct (OMCD),[2] have the highest rate of acid secretion among the distal tubule segments and are therefore essential to the maintenance of acid base balance (2).

The gastric parietal cell is the site of generation of acid and bicarbonate through the action of cytosolic carbonic anhydrase II (5, 6). The intracellular acid is secreted into the lumen via gastric H-K-ATPase, which works in conjunction with a chloride channel and a K^+ recycling pathway (7–10). The intracellular bicarbonate is transported to the blood via basolateral Cl^-/HCO_3^- exchangers (11–14).

SLC26 (human)/Slc26 (mouse) isoforms are members of a conserved family of anion transporters that display tissue-specific patterns of expression in epithelial cells (15–24). Several SLC26 members can function as chloride/bicarbonate exchangers. These include SLC26A3 (DRA), SLC26A4 (pendrin), SLC26A6 (PAT1 or CFEX), SLC26A7, and SLC26A9 (25–31). SLC26A7 and SLC26A9 can also function as chloride channels (32–34).

SLC26A7/Slc26a7 is predominantly expressed in the kidney and stomach (28, 29). In the kidney, Slc26a7 co-localizes with AE1, a well-known Cl^-/HCO_3^- exchanger, on the basolateral membrane of (acid-secreting) A-intercalated cells in OMCD cells (29, 35, 36) (supplemental Fig. 1). In the stomach, Slc26a7 co-localizes with AE2, a major Cl^-/HCO_3^- exchanger, on the basolateral membrane of acid secreting parietal cells (28). To address the physiological function of Slc26a7 in the intact mouse, we have generated Slc26a7 ko mice. We report here that Slc26a7 ko mice exhibit distal renal tubular acidosis and impaired gastric acidification in the absence of morphological abnormalities in kidney or stomach.

EXPERIMENTAL PROCEDURES

Preparation of Slc26a7-null Targeting Construct, ES Electroporation, Chimeric Mice Generation, PCR Screening of F1 Pups (Germline Transmission), and Generation of Slc26a7-null Mice—Our strategy was to delete the Slc26a7 gene by knocking out exons 3 and 4, which encode 168 amino acid residues. Toward this end, a ~15.6-kb fragment was subcloned from the BAC-encoding part of the Slc26a7 gene for generation of a targeting construct. The construct was designed with the short homology arm (SA) extending ~2.0-kb 5′ to exon 3, and with the long homology arm (LA) extending 8.3 kb 3′ beyond the 3′-end of exon 4. The Neo cassette replaces 4.2 kb of the gene including exons 3 and 4. Each modification step in construction of the targeting vector was confirmed by

* This work was supported, in whole or in part, by a Merit Review award from the Department of Veterans Affairs (to M. S.) and National Institutes of Health Grants DK62809 (to M. S.) and DK 43495 (to S. L. A.). This work was also supported by the Deutsche Forschungsgemeinschaft Sachbeihilfe Se 460/9-5 and 9-6 and Ministry of Science in Lower Saxony (to U. S.), and by grants from the DCA dialysis care group (to M. S.).

[S] The on-line version of this article (available at http://www.jbc.org) contains supplemental "Results" and Figs. 1–4.

[1] To whom correspondence should be addressed: Center on Genetics of Transport and Epithelial Biology and Dept. of Medicine, University of Cincinnati, 231 Albert Sabin Way, MSB G259, Cincinnati, OH 45267-0585. Fax: 513-558-4309; E-mail: Manoocher.Soleimani@uc.edu.

[2] The abbreviations used are: OMCD, outer medullary collecting duct; ko, knockout; LA, long homology arm; SA, short homology arm.

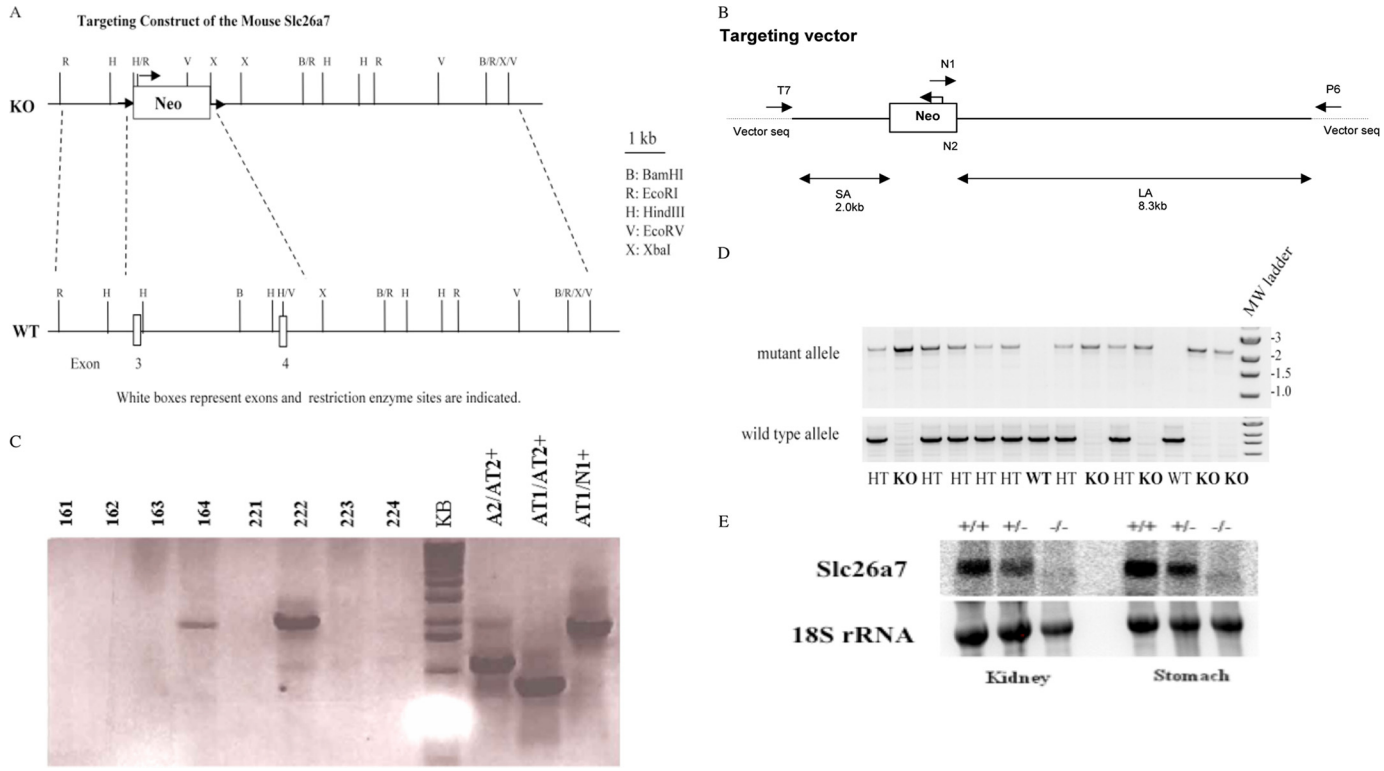

FIGURE 1. **Generation of Slc26a7$^{-/-}$ mutant mice.** *A*, schematic diagram of the Slc26a7 targeting construct. The Neo cassette replaces 4.0 kb of the gene including exons 3 and 4. *B*, Slc26a7 targeting allele and delineation of the locations of primers. Using primers designated as A1, A2, and A3, which are downstream (3′) to the SA, PCR reactions were performed in conjunction with a primer at the 5′-end of the Neo cassette (referred to as *N1*). These reactions were expected to amplify 2.1-, 2.2-, and 2.3-kb fragments, respectively. The control PCR reaction was done using AT1 and AT2, which is at the 5′-end of the SA inside the region used to create the targeting construct. This amplifies a band of 2.0 kb. *C*, identification of homologous recombinant clones. PCR analysis of DNA isolated from 200 surviving colonies identified two individual clones, which showed homologous recombination. Southern blotting confirmed the results. The positive control was performed using primers AT1/N1, which gave the expected fragment size of 1.8 kb. *D*, generation of Slc26a7$^{+/+}$ and Slc26a7$^{-/-}$ mice. Tail DNA genotyping identified Slc26a7+/+, +/−, and −/− mice. *E*, expression of Slc26a7 in kidney and stomach. Crossing of male and female heterozygote mice (+/−) resulted in the generation of Slc26a7 ko (−/−) mice. Northern hybridization on RNA isolated from kidneys and stomachs of Slc26a7 +/+, +/−, and −/− mice indicated that the expression of Slc26a7 is completely absent in Slc26a7-null mouse. Both male and female Slc26a7$^{-/-}$ mice were fertile.

restriction analysis and by sequencing using primers designed to read from the selection cassette into the LA and the SA. T7 and P6 primers anneal to the vector sequence and read into the 5′- and 3′-ends of the BAC subclone. The schematic diagram in Fig. 1*A* depicts the targeting construct used to generate the Slc26a7 ko mouse, with location of the Neo cassette indicated.

10 μg of the targeting vector were linearized by AscI and used to transfect 129/SV embryonic stem cells by electroporation. After selection in G418, surviving clones were expanded for PCR analysis to identify recombinant ES clones. Primers A1, 2, and 3 were designed downstream (3′) to the short homology arm (SA) outside the region used to generate the targeting construct (Fig. 1*B*). PCR reactions using A1, 2, or 3 with the N1 primer at the 5′-end of the Neo cassette amplify 2.15, 2.18, and 2.25 kb fragments, respectively. The control PCR reaction was performed using AT1 and AT2, which is at the 5′-end of the SA inside the region used to create the targeting construct. This amplifies a band of 1.6 kb. The oligo sequences used to screen the ES clones were as follows: A1: 5′-attccctggaacttcagttcc-3′; A2: 5′-actctgattagtgcattcctc-3′. A3: 5′-ttggac acagccattcatgc-ctg-3′; AT1: 5′-aggaccaggaagttctctcag-3′. AT2: 5′-gcatggc-aatctctgagttcagtc-3′; N1: 5′-tgcga ggccagagg ccacttgtgtagc-3′.

Individual clones were screened with A2/N1 primers. Fig. 1*C* is a PCR analysis of DNA isolated from ES cells after electroporation with the targeting construct and selection with G418. More than 400 surviving colonies were screened. As shown in Fig. 1*C*, at least two clones (clones 164 and 222) were identified as having undergone homologous recombination. The positive control amplifications using primers A2/AT2, AT1/AT2, and AT1/N1 gave the expected fragment sizes of 1.1, 0.8, and 1.8 kb, respectively. The homologous recombination events in clones 164 and 222 were further validated by Southern blot (data not shown).

ES cells from clones 164 or 222 were microinjected into C57BL/6J blastocysts. Chimeric mice were bred to obtain wild-type (Slc26a7$^{+/+}$) and heterozygous (Slc26a7$^{+/-}$) mice (Fig. 1*D*). Intercrossing of Slc26a7 heterozygotes (+/−) generated Slc26a7 ko mice. Tail DNA genotyping was performed using the A2/N1 primer set (see above). Northern hybridization demonstrated the complete absence of Slc26a7 mRNA in stomach and kidney of Slc26a7-null mice (Fig. 1*E*). Immunofluorescence labeling in kidney and stomach verified the absence of Slc26a7 in −/− mice (data not shown). Slc26a7-null mice are healthy and have normal blood pressure.

Animals—Mice were cared for in accordance with the Institutional Animal Care and Use Committee (IACUC) at the University of Cincinnati and the Medical School of Hannover University. All animal handlers were IACUC-trained. Animals had access to food and water *ad libitum*, were housed in humidity, temperature and light/dark-controlled rooms, and were

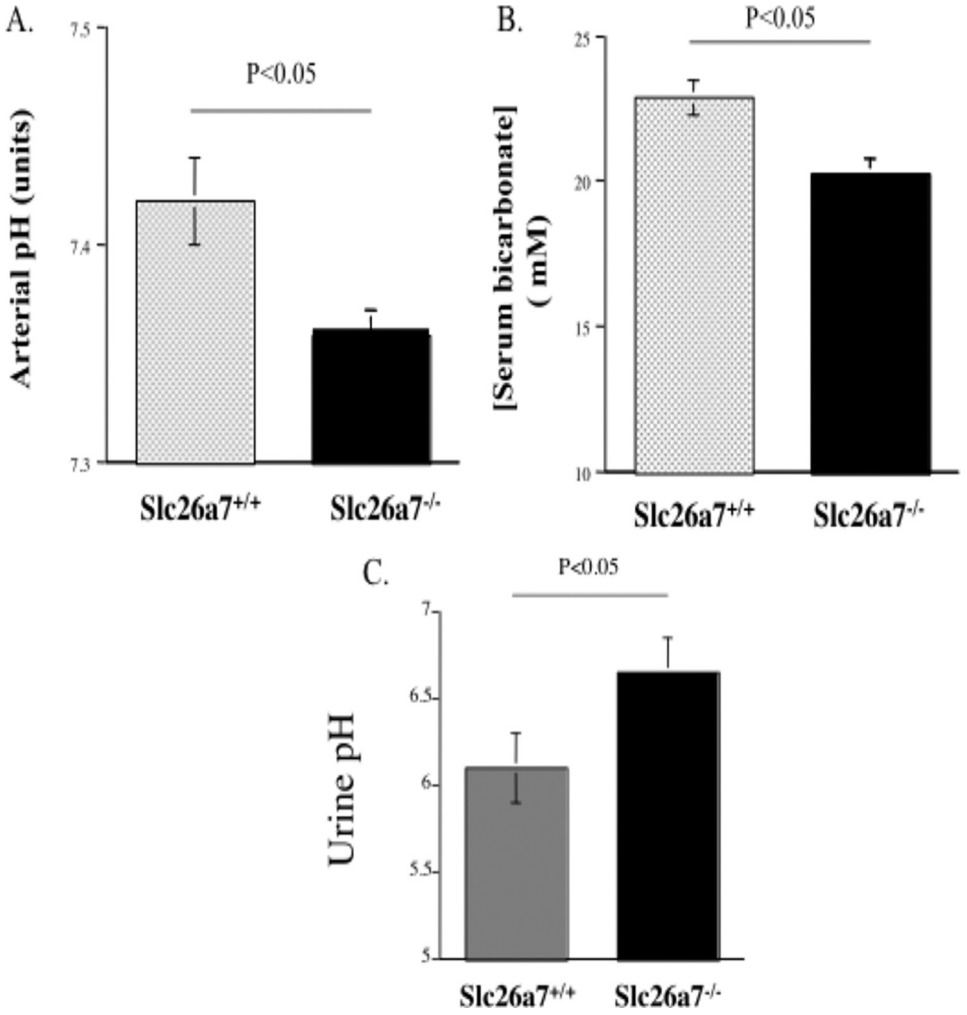

FIGURE 2. **Slc26a7$^{-/-}$ mice have distal renal tubular acidosis.** *A* and *B*, arterial blood gas and serum bicarbonate. Arterial blood gas and serum chemical analysis demonstrated a significant reduction in arterial pH, and serum bicarbonate, consistent with metabolic acidosis in Slc26a7$^{-/-}$ mice. *C*, urine pH. Slc26a7 ko mice have elevated urine pH despite presence of metabolic acidosis.

inspected daily. Animals were euthanized with the use of either anesthetics (pentobarbital sodium) or cervical dislocation after carbon dioxide narcosis according to institutional guidelines and approved protocols.

In Vitro Microperfusion of Kidney Tubules and Measurement of Basolateral Cl^-/HCO_3^- Exchanger Activity in Acid-secreting Cells in the OMCD—Kidneys from wild-type and Slc26a7-null mice were decapsulated, sectioned into three to four cross sections per kidney, and immediately placed in a Petri dish containing dissecting solution. Each section was stripped from the papillary tip to the cortex into smaller wedges and transferred into a second Petri dish containing dissecting solution maintained at 14 °C under a dissecting microscope (Nikon SMZ-645). Segments of OMCD were dissected and microperfused as before (3, 38). The perfusate and bath superfusate were equilibrated with solutions containing 95% O_2-5% CO_2. After equilibration, the tubule was luminally perfused for 5 min with 5 μM of the pH-sensitive dye BCECF-AM, leading to uptake of dye by intercalated cells only, and not by principal cells (39). Fluorescent measurements were done with ratio digital imaging system using an inverted fluorescence microscope (Nikon TE-300). Excitation wavelengths were recorded at 490 and 440 nm, and emission was measured at 520 nm. Only one tubule per animal was examined, with the visual field including two to four cells per tubule. Intracellular calibration was performed by using the high-K^+-nigericin method (3, 38, 42).

Basolateral Cl^-/HCO_3^- exchanger activity in Type A-ICs was assessed as the rate of pH_i change, as well as the amplitude of pH_i response when the bath perfusate was switched to a Cl^--free solution. This maneuver causes cell alkalinization in Type A-ICs via reversal of the basolateral Cl^-/HCO_3^- exchanger. Following pH_i stabilization in Cl-free medium, the bath perfusate was switched back to a Cl^--containing solution, resulting in recovery of pH_i to baseline levels via Cl^-/HCO_3^- exchange (3, 38, 42).

Measurement of Acid Secretory Rate in Isolated Gastric Mucosa—The experimental maneuvers were similar to those published, with modifications as described (10). Briefly, the mucosal layer was dissected from mouse gastric corpus under a stereomicroscope and mounted between two Lucite half chambers of a water-jacketed Ussing system equipped with a gas-lift system. The exposed surface area was 0.283 cm^2. The serosal solution contained (in mM) 108 NaCl, 22 $NaHCO_3$, 3 KCl, 1.3 $MgSO_4$, 2 $CaCl_2$, 2.25 KH_2PO_4, 8.9 glucose, and 10 sodium pyruvate and was gassed with 95% O_2-5% CO_2, pH 7.4. The chamber was allowed to equilibrate for at least 30 min in the presence of indomethacin (3×10^{-5} M) and tetrodotoxin 10^{-6} M) added to the serosal solution to minimize the impact of intrinsic prostanoid and neural tone.

The mucosal solution (154 mM NaCl) was gassed with 100% O_2 and maintained at pH 7.4 by the controlled addition of dilute (2 mM) NaOH (in 0.1-μl volume) using a pH-Stat titration system (Radiometer, Copenhagen, Denmark). If the stomach showed acid secretion, basal parameters were measured for 30 min; and, after addition of 10^{-5} M forskolin to serosal solution, a maneuver known to stimulate acid secretion. Acid secretory rates were recorded for 60 min at 5-min intervals. Data represent means ± S.E.

RESULTS

Generation of Slc26a7-null Mice—The Neo cassette replaces 4.0 kb of the gene including exons 3 and 4 (Fig. 1, *A* and *B*, "Experimental Procedures"). Targeted ES cells (Fig. 1*C*) were

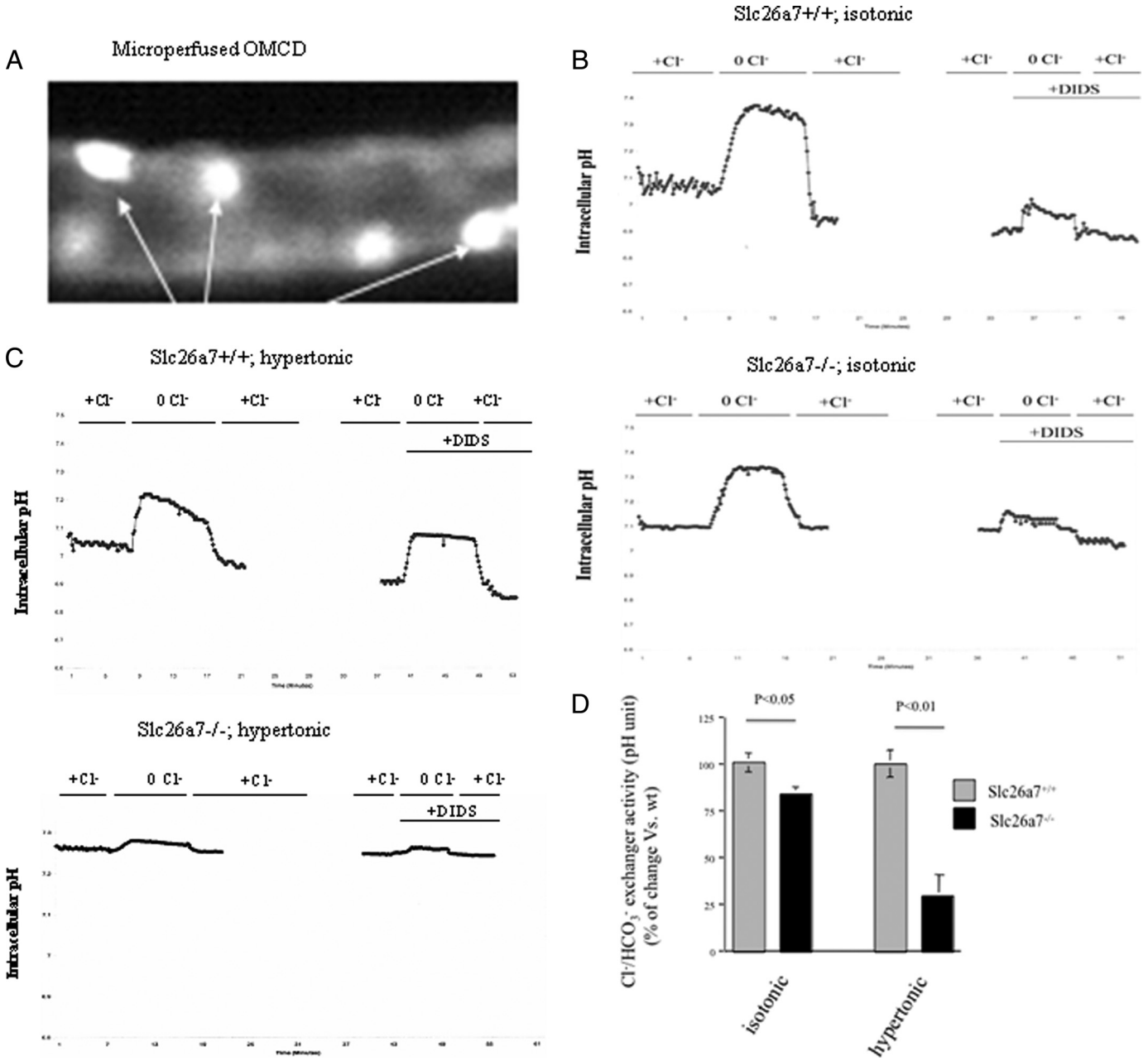

FIGURE 3. **Basolateral Cl^-/HCO_3^- exchanger in acid (*A*)-intercalated cells in OMCD.** *A*, microperfused mouse kidney OMCD. The acid-secreting (*A*)-intercalated cells are delineated by high fluorescence intensity reflecting cell type-specific BCECF uptake. *B*, representative intracellular pH (pH_i) tracing of an individual A-intercalated cell of OMCD in isotonic solution. Tubules from Slc26a7$^{+/+}$ (*left panel*); Slc26a7$^{-/-}$ mice (*right panel*) were subjected to sequential chloride removal and restoration, first in the absence and then in the presence of DIDS (10 μM). *C*, representative intracellular pH (pH_i) tracing of an individual A-intercalated cell of OMCD in hypertonic solution subjected to the same protocol. Slc26a7$^{+/+}$ (*left panel*); Slc26a7$^{-/-}$ (*right panel*). *D*, rate of intracellular alkalinization in response to basolateral Cl^- removal in A-intercalated cells in isotonic and hypertonic solutions. As shown, basolateral Cl^-/HCO_3^- exchanger activity is significantly decreased in Slc26a7$^{-/-}$ in a hypertonic solution.

used to generate chimeric mice that were bred to obtain wild-type (Slc26a7$^{+/+}$), heterozygous (Slc26a7$^{+/-}$), and null (Slc26a7$^{-/-}$) mice (Fig. 1*D*). The expression of Slc26a7 was completely abrogated in the kidney and stomach of Slc26a7-null mice (Fig. 1*E*). Slc26a7$^{-/-}$ mice exhibited normal growth, blood pressure, and survival relative to wild-type littermates.

Slc26a7-null Mice Have Distal Renal Tubular Acidosis—Arterial blood gas analysis and blood chemistry examination demonstrated a significant reduction in arterial pH and serum bicarbonate, consistent with metabolic acidosis (Fig. 2, *A* and *B*, $n = 13$ in each group). Slc26a7 ko mice have elevated urine pH (Fig. 2*C*), despite severe metabolic acidosis (Fig. 2, *A* and *B*). The presence of metabolic acidosis, along with an inappropriately alkaline urine pH, is indicative of distal renal tubular acidosis in Slc26a7 ko mice. Urine output was 2.01 ± 0.2 and 1.92 ± 0.2 ml/24 h in Slc26a7$^{+/+}$ and Slc26a7$^{-/-}$ mice, respectively ($p > 0.05$, $n = 5$ in each group). Urine osmolarity was 2489 ± 180 and 2710 ± 150 mosm/liter in Slc26a7$^{+/+}$ and Slc26a7$^{-/-}$ mice, respectively ($p > 0.05$, $n = 5$ in each group).

When challenged with an acid load in the form of NH_4Cl (at 280 mM) added to their drinking water for seven days, Slc26a7$^{+/+}$ and Slc26a7$^{-/-}$ mice dropped their serum bicar-

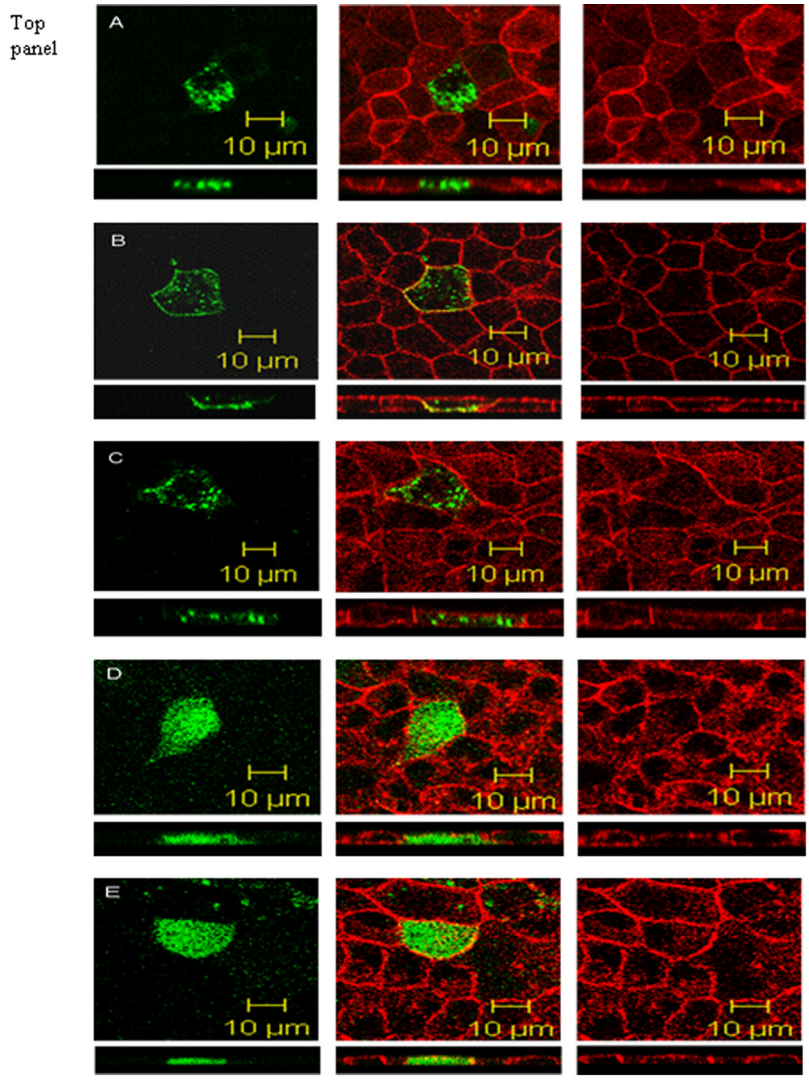
Top panel
A
B
C
D
E
10 μm

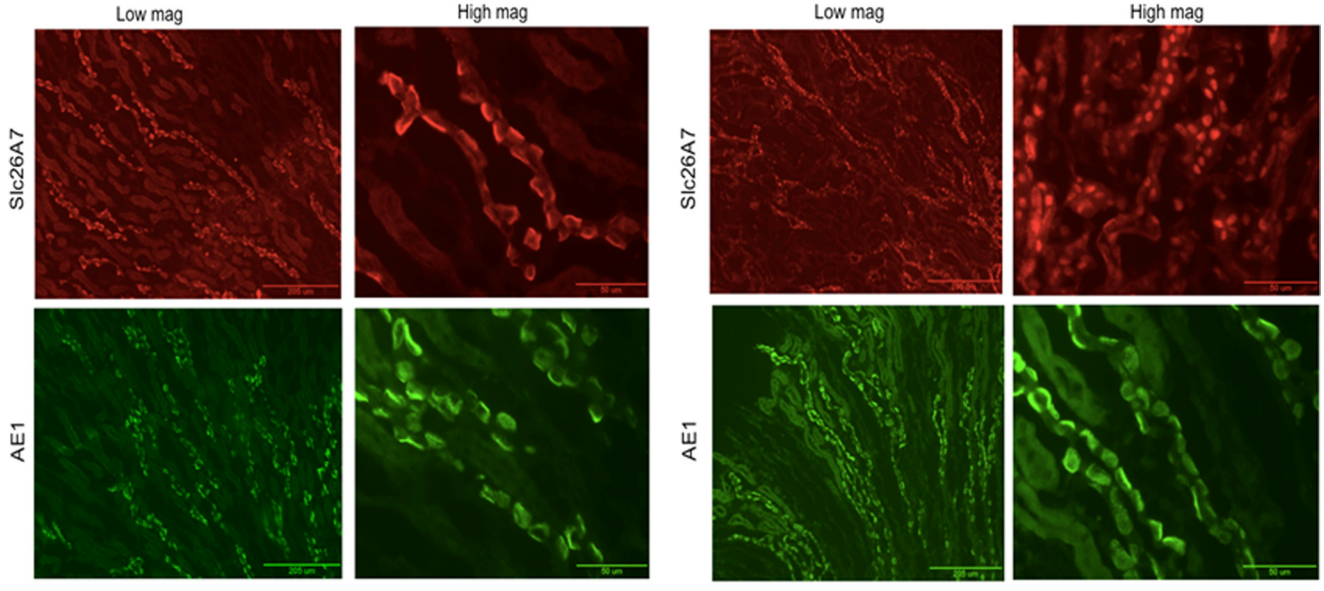
Bottom panel
A. Control
B. Water loading
Low mag
High mag
Slc26A7
AE1

bonate to 21 ± 1 and 15.5 ± 1 mEq/liter, respectively ($p < 0.01$, $n = 5$). Urine pH was ~5.5 and 6.5 in Slc26a7$^{+/+}$ and Slc26a7$^{-/-}$ mice, respectively, following challenge with the acid load ($p < 0.05$). These results demonstrate a more profound drop in serum bicarbonate (~4.5 mEq/liter *versus* 1.7 mEq/liter, $p < 0.05$, $n = 5$) and the inability to acidify urine pH (6.5 *versus* 5.5, $p < 0.05$) in response to acid load in Slc26a7 ko mice. Taken together, these results are consistent with distal renal tubular acidosis in Slc26a7-null mice.

Impaired Basolateral Cl^-/HCO_3^- Exchanger Activity in Acid-secreting (A) Intercalated Cells in the OMCD—Given the localization of Slc26a7, we next examined the functional activity of the basolateral chloride/bicarbonate (Cl^-/HCO_3^-) exchanger in acid-secreting cells in the OMCD. Toward this end, intracellular pH in A-intercalated cells was measured by the pH-sensitive dye (BCECF) in microperfused kidney outer medullary collecting duct (OMCD). Fig. 3*A* depicts a microperfused mouse kidney OMCD. The acid-secreting (A) intercalated cells are delineated by bright color, which reflects the uptake of BCECF, as principal cells do not take up the dye in significant amount. Fig. 3*B* (left) is a representative pH_i tracing in Slc26a7$^{+/+}$ mouse OMCD and performed in isotonic solutions (290 mosM) in the perfusate and bath. As indicated, there is a significant intracellular alkalinization in response to the removal of bath chloride in microperfused OMCD, which is significantly diminished in the presence of 10 μM DIDS (Fig. 3*B*, *left*). Fig. 3*B* (*right*) depicts pH_i tracing in Slc26a7$^{-/-}$ mouse OMCD and indicates the presence of a significant DIDS-sensitive intracellular alkalinization in response to the removal of bath chloride in microperfused OMCD. Fig. 3*C* (*left*) is a representative pH_i tracing in Slc26a7$^{+/+}$ mouse OMCD and performed in hypertonic (440 mosM) perfusate and bath (mannitol was used to make the solutions hypertonic). As indicated, there is a significant intracellular alkalinization in response to the removal of bath chloride in microperfused OMCD cells, which is not significantly affected by 10 μM DIDS (Fig. 3*C*, *left*). The rate of the intracellular alkalinization in hypertonic solution is significantly diminished in Slc26a7$^{-/-}$ mice (Fig. 3*C*, *left versus right panel*). In all experiments that were performed in either isotonic or hypertonic medium, EIPA at 10 μmol was added to the bath to prevent NHE1 activation and potassium was removed from the luminal fluid and concanamycin A at 100 nM added to the lumen to inactivate H-K-ATPase and H^+-ATPase, respectively. The baseline pH_i was significantly elevated in hypertonic medium in Slc26a7$^{-/-}$ mice (pH_i 7.26) *versus* Slc26a7$^{+/+}$ animals (pH_i 7.11) (Fig. 3*C*). The results of five separate experiments from different animals demonstrated that the rate of basolateral Cl^-/HCO_3^- exchange was decreased by only ~18% in Slc26a7$^{-/-}$ in isotonic medium ($p < 0.05$) but decreased by >70% in hypertonic medium relative to Slc26a7$^{+/+}$ mice ($p < 0.01$) (Fig. 3*D*). Whether the set point for other basolateral acid base transporters is changed in hypertonic medium in Slc26a7 ko mice cannot be excluded.

Decreasing the Osmolarity of the Medium Decreases the Membrane Abundance of Slc26a7 in Vitro—The osmotically tolerant cultured kidney (MDCK) cells were transiently transfected with the epitope-tagged Slc26a7 (referred to GFP-Slc26a7) and switched to a hypertonic medium (440 mM) overnight to mimic the *in vivo* milieu in the medulla. Forty-eight hours after transfection, cells were either switched to an isotonic medium or remained in hypertonic medium for an additional 60 min. Cells were then fixed and processed for image analysis under confocal microscopy. The results as demonstrated in Fig. 4, *top panel* indicate that reducing the osmolarity of the medium from hypertonic (440 mM) to isotonic (290 mM) for 60 min, which mimics the changes in microperfused OMCD (Fig. 3), causes significant reduction in membrane abundance of Slc26a7 (Fig. 4, *top panel*, *column C*) relative to cells that stay in hypertonic medium, which demonstrate a predominant membrane expression pattern (Fig. 4, *top panel*, *column B*). The Z-line (side view) images of confocal pictures demonstrate that the membrane abundance of Slc26a7 is indeed decreased in cells switched to isotonic medium (Fig. 4, *top panel*, lower frame of column C relative to column B). The epitope-tagged Slc26a7 was predominantly detected in the cytoplasm in cells transfected and grown in isotonic medium (Fig. 4, *top panel*, *column A*). The GFP alone (no Slc26a7 insert) was localized intracellularly in both isotonic and hypertonic medium (Fig. 4, *top panel*, *columns D* and *E*). The membrane abundance of epitope-tagged AE1 did not change in isotonic medium (data not shown).

Decreasing the Osmolarity of the Medulla in Vivo Reduces the Membrane Abundance of Slc26a7 in OMCD Cells—To reduce medullary osmolarity, animals were subjected to water loading according to established protocols. Briefly, the control group was allowed tap water *ad libitum*; whereas, the water-loaded animals were induced to drink water abundantly by adding glucose (50 g/1000 ml) to their drinking water. This maneuver has been shown to increase water intake, decrease urine osmolarity and increase urine output, all indicators of decreasing medullary interstitial osmotic gradient. Our *in vivo* studies confirmed the *in vitro* findings in Fig. 4, *top panel*, by demonstrating that

FIGURE 4. **Effect of osmolarity on Slc26a7 expression *in vivo* and *in vitro*.** *Top panel*, transient transfection of epitope-tagged Slc26a7 in cultured kidney (MDCK) cells: effect of decreasing tonicity. Cells were transiently transfected with the GFP-SLC26A7 construct in isotonic medium and 24 h later were either exposed to a hypertonic (440 mM) medium or remained in isotonic (290 mM) medium. *Top panel*, *A*, cells incubated in isotonic medium for the duration of transient transfection (48 h) show intracellular localization of Slc26a7. *B* and *C*, cells were transfected with GFP-Slc26a7 in isotonic medium and switched to a hypertonic medium 24 h later. 24 h after switching to the hypertonic medium, cells were either switched back to an isotonic (290 mM) medium (*column C*) or remained in hypertonic medium (*column B*) for an additional 60 min. Cells were fixed and analyzed under confocal microscopy. *D* and *E*, cells transfected with the GFP alone (no SLC26A7) and grown in isotonic or hypertonic medium are detected in the cytoplasm (*columns D* and *E*). Z-line (*side view*) images of confocal pictures (*lower frame* for each column) demonstrate that Slc26a7 is detected predominantly in the basolateral membrane in hypertonic medium (*top panel*, *column B*) and intracellularly in isotonic medium either for 48 h (*top*, *column A*) or 60 min after being switched back from hypertonic medium (*top panel*, *column C*). Frames under each column show side view images. *Bottom panel*, effect of reduced medullary osmolarity on membrane abundance of Slc26a7 and AE1 in OMCD. Animals were subjected to water loading for 5 days by addition of glucose to their drinking water. Kidney sections from animals with hypertonic medulla (control) or reduced osmolarity (water-loaded) were immunostained with Slc26a7 or AE1 antibodies. *Bottom panel*, *section A*, Slc26a7 and AE1 staining in control state. *Bottom panel*, *section B*, Slc26a7 and AE1 in water-loaded animals. Slc26a7 shows significant reduction in membrane abundance in water-loaded animals.

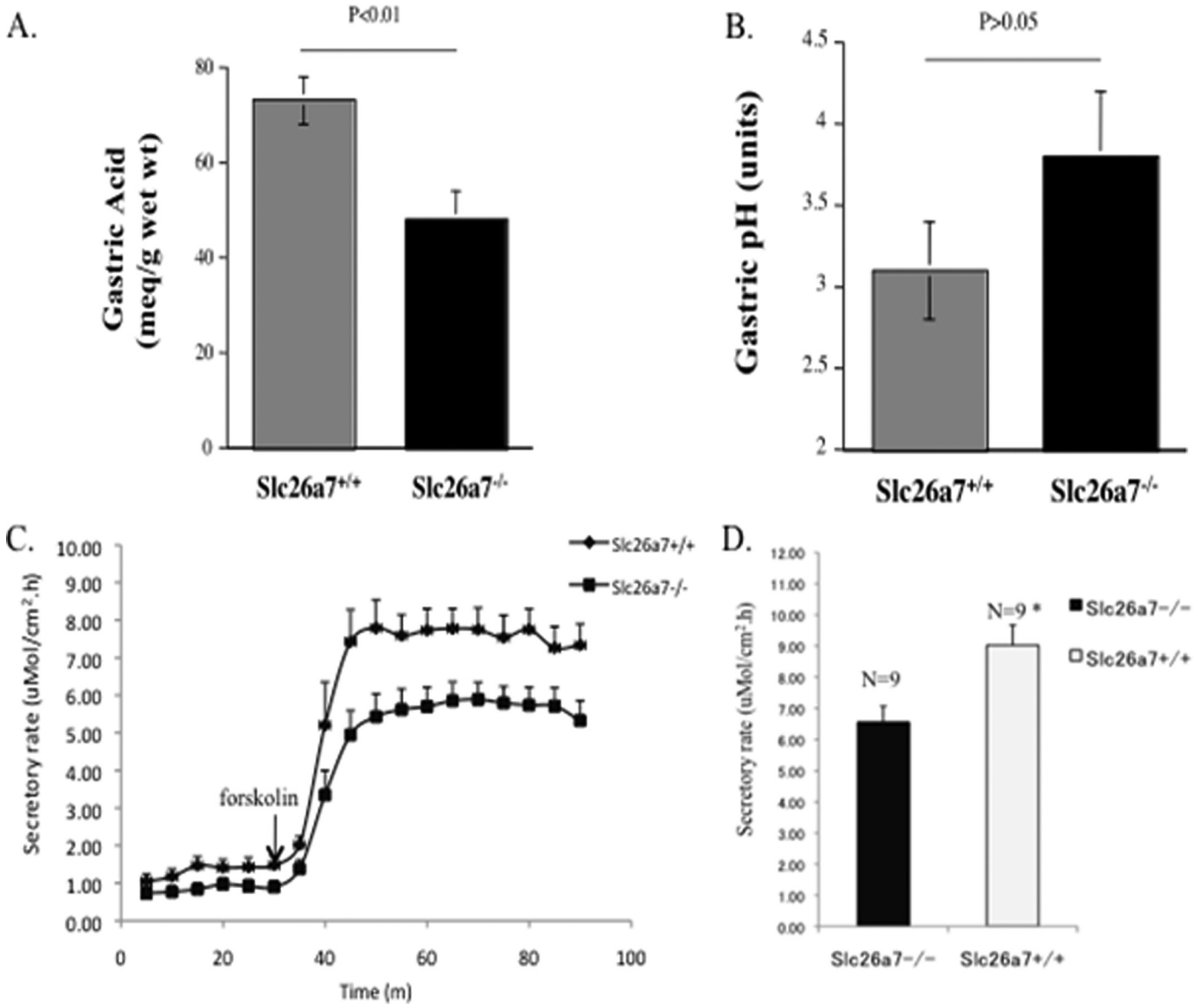

FIGURE 5. **Gastric acid secretion in Slc26a7$^{+/+}$ and Slc26a7$^{-/-}$ mice.** Animals 5–6 weeks old were fasted overnight and injected subcutaneously with histamine at 2 μg/g body weight. After 15 min, the intact stomach was removed. The gastric contents, which included both basal and histamine-stimulated acid-base equivalents, were rinsed in 5 ml of normal saline solution and centrifuged. Total acid-base equivalents in the supernatant were determined by titration with NaOH. *A*, gastric acid secretion in Slc26a7$^{+/+}$ and Slc26a7$^{-/-}$ mice. Total secreted acid was decreased by ~36% in Slc26a7$^{-/-}$ *versus* Slc26a7$^{+/+}$ mice. *B*, gastric pH in Slc26a7$^{+/+}$ and Slc26a7$^{-/-}$ mice. The pH of the gastric secretions was more alkaline in Slc26a7$^{-/-}$ mice. *C* and *D*, acid secretory rates in isolated gastric mucosa of adult Slc26a7$^{-/-}$ and Slc26a7$^{+/+}$ mice. *C*, acid secretion was measured at basal state and following the stimulation with forskolin (10^{-5} M) in gastric mucosa of 40–45 days old (*left* and *right panels*). *D*, peak secretory acid secretion was decreased in Slc26a7$^{-/-}$ mice relative to Slc26a7$^{+/+}$ mucosa ($n = 6$ for +/+, 7 for −/− mice).

decreasing the tonicity of the kidney medulla by water loading reduced the membrane abundance of Slc26a7 in A-intercalated cells in the OMCD (Fig. 4, *bottom panel*, *section B*). Interestingly, the abundance of AE1 was not significantly affected in water loading (Fig. 4, *bottom panel*, *section B*).

Impaired Gastric Acid Secretion in Slc26a7-null Mice—To ascertain the role of Slc26a7 in gastric acid secretion, stomach pH and amount of acid in gastric secretions from Slc26a7$^{+/+}$ and Slc26a7$^{-/-}$ mice were examined following stimulation of acid secretion with histamine. The pH of gastric secretions was not significantly different in Slc26a7$^{-/-}$ mice, with values of 4.2 ± 0.4 in Slc26a7$^{-/-}$ mice *versus* 3.5 ± 0.4 in Slc26a7$^{+/+}$ (Fig. 5*A*, $p > 0.05$). Quantitation of gastric acid revealed acid secretion to be significantly decreased in Slc26a7$^{-/-}$ mice (75 ± 6 mEq/g wet weight in Slc26a9$^{+/+}$ and 46 ± 4 in Slc26a7$^{-/-}$ mice) (Fig. 5*B*, $p < 0.01$).

Acid Secretion in Isolated Gastric Mucosa from Adult Mice—To quantify actual rates of HCl secretion, isolated gastric mucosae from Slc26a7$^{+/+}$ and Slc26a7$^{-/-}$ mice were studied in modified Ussing-chamber systems. The gastric mucosa from Slc26a7$^{-/-}$ mice 40–45 days of age showed significant impairment in forskolin-stimulated acid secretion compared with that of wt mice (Fig. 5*C*, *left* and *right panels*; summarized in Fig. 5*D*).

DISCUSSION

Our studies in osmotically tolerant cultured kidney (MDCK) cells demonstrate that reducing the osmolarity of the medium from hypertonic (440 mM) to isotonic (290 mM) for 60 min,

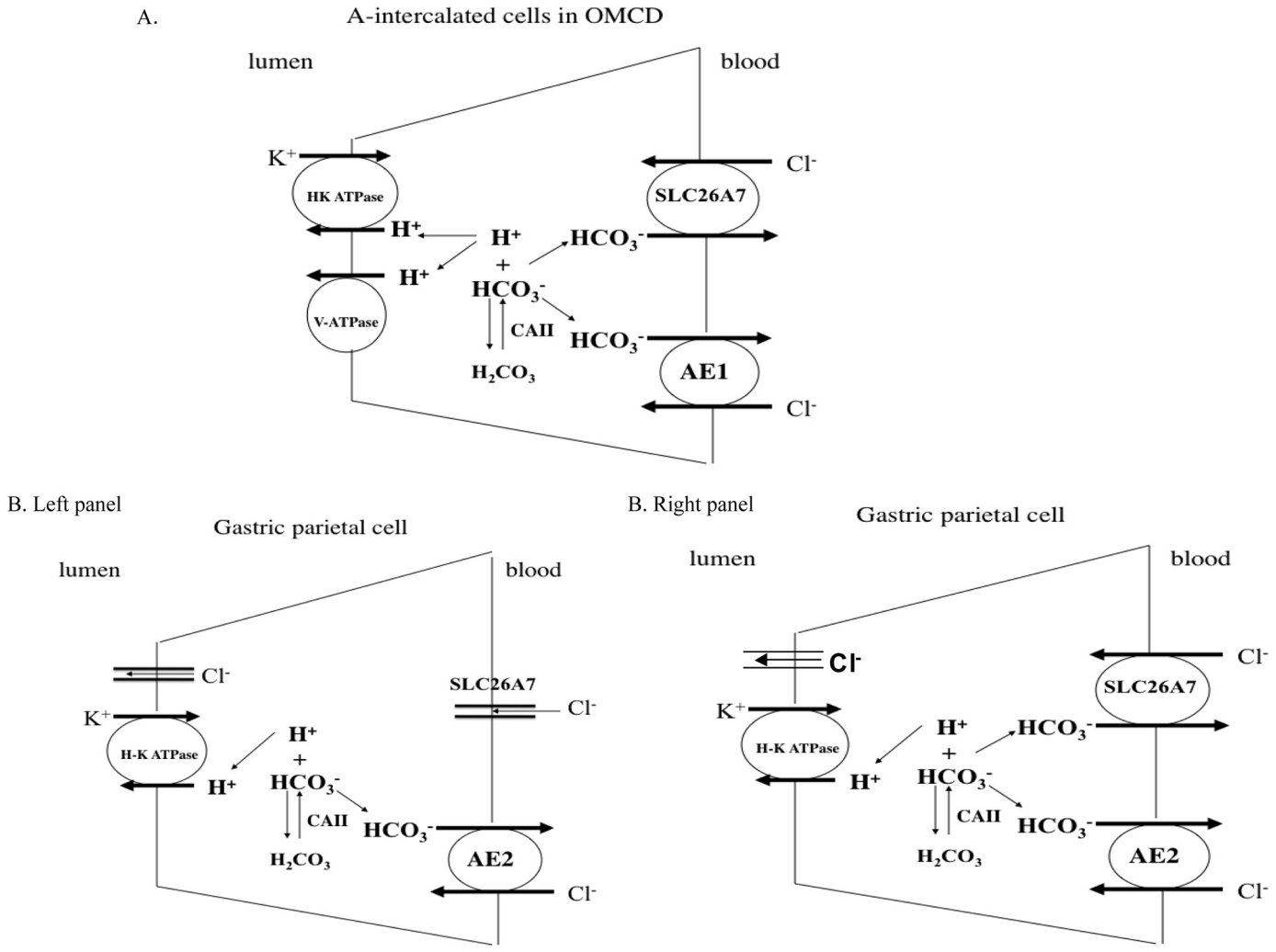

FIGURE 6. **Schematic diagrams depicting Slc26a7 as a major regulator of acid secretion in the kidney outer medullary collecting duct (*A*) and stomach parietal cells (*B*).** *A*, Slc26a7 and AE1 co-localize on the basolateral membrane of acid-secreting intercalated cells in the OMCD. Slc26a7 is predominantly active in hypertonic environment whereas AE1 can function better at isotonic or hypotonic environment. *B*, Slc26a7 can regulate acid secretion in the stomach by either functioning as a Cl^-/HCO_3^- exchanger (*right panel*) or an chloride channel (*left panel*) on the basolateral membrane of gastric parietal cells.

which mimics the changes in perfused OMCD (Fig. 2), causes significant endocytosis of Slc26a7 from the membrane to the cytoplasm (Fig. 4, *top panel*). These results are in agreement with our previously published reports demonstrating that the membrane abundance of Slc26a7 in significantly increased in hypertonic medium by increasing its trafficking from the cytosolic pool (35, 36). The membrane abundance of epitope-tagged AE1 was not affected by changes in the medium tonicity of medulla.[3]

Our *in vivo* studies confirmed the *in vitro* findings by demonstrating that decreasing the tonicity of kidney medulla by water loading reduced the membrane expression of Slc26a7 but had no significant effect on the abundance of AE1 in the basolateral membrane of A-intercalated cells in the OMCD (Fig. 4, *bottom panel*, *section B*). The expression pattern of Slc26a7 and AE1 in control state is shown for comparison (Fig. 4, *bottom panel*, *section A*). Further, increasing the osmolarity of the medulla by water deprivation was associated with the increased abundance of Slc26a7 and decreased abundance of AE1 in the plasma membrane of A-intercalated cells in OMCD (36). Taken together, these studies indicate that Slc26a7 is the dominant bicarbonate-extruding transporter in the OMCD in hypertonic medium; whereas, AE1 is more active in isotonic environment. Northern hybridization and immunohistochemistry studies indicated enhanced expression of AE1 in the OMCD of Slc26a7-null mice (supplemental Fig. 2). The expression of pendrin, the apical Cl^-/HCO_3^- exchanger in B-intercalated cells, was significantly decreased in Slc26a7-null mice (supplemental Fig. 2).

Mutations in AE1 have been shown to be associated with distal renal tubular acidosis, as manifested by metabolic acidosis and renal bicarbonate wasting (4). AE1 is expressed on the basolateral membrane of acid-secreting (Type A) intercalated cells in the cortical, outer medullary and the first segment of the inner medullary collecting duct (1–4, 37–39). Systemic deletion of AE1 in mouse is associated with severe spherocytic hemolytic anemia and early lethality, in some cases due to widespread thrombosis (40). The examination of the kidney defect in systemic AE-1 ko mice is therefore complicated by the presence of concurrent severe systemic perturbations that can

[3] J. Xu and M. Soleimani, unpublished data.

impact the kidney medulla and indirectly affect the activity of ion transporters. However, surviving AE-1-null mice exhibit only a 25% reduction in Cl^-/HCO_3^- exchanger activity in Type A-intercalated cells of the OMCD (41) as measured in an isotonic environment.

Slc26a7 ko mice displayed reduced gastric acid secretion (Fig. 5). Functional studies in cultured cells or oocytes demonstrated that Slc26a7 can function as a chloride channel, as well as a Cl^-/HCO_3^- exchanger (28, 29, 32–34). As a Cl^-/HCO_3^- exchanger, Slc26a7 can facilitate the extrusion of bicarbonate across the basolateral membrane, which should enhance the generation of intracellular acid for secretion into the stomach lumen via apical H-K-ATPase. As a chloride channel, Slc26a7 can contribute to the transport of chloride from blood into parietal cells for eventual secretion across the apical membrane along with the acid (H^+). In either mode, Slc26a7 has the potential to regulate gastric acid secretion, albeit via different mechanisms. Whether the main functional mode of Slc26a7 in gastric parietal cells is the mediation of Cl^-/HCO_3^- exchange or chloride channel remains speculative. Our studies in isolated gastric mucosa mounted on Ussing chamber (Fig. 5) do not distinguish between the two possible functional modes of Slc26a7.

Slc26a7 co-localizes with AE2 (Slc4a2), a known Cl^-/HCO_3^- exchanger, on the basolateral membrane of gastric parietal cells (28). Systemic deletion of AE2 resulted in growth retardation along with achlorhydria (13, 14). Histological studies revealed abnormalities of the gastric epithelium, including moderate dilation of the gastric gland lumens and a reduction in the number of parietal cells in AE2-null mice (13, 14). The expression of Slc26a7 was significantly deceased in stomachs of AE2-null mice (13). Ultrastructural analysis of $AE2^{-/-}$ gastric mucosa indicated loss of secretory canaliculi and tubulovesicles (13). These results demonstrate that AE2 is essential for maintaining the viability or development of parietal cells and for normal abundance of secretory canalicular and tubulovesicular membranes in mouse parietal cells. Whether the achlorhydria in AE2-null mice is partly due to the down-regulation of Slc26a7 needs further investigation. We did not observe any detectable alteration in the expression of AE2 on the basolateral membrane of gastric parietal cells in Slc26a7-null mice (supplemental Fig. 3). Stomach and kidney histology in $Slc26a7^{-/-}$ did not differ from those of $Slc26a7^{+/+}$ mice (supplemental Fig. 4).

In conclusion, genetic deletion of Slc26a7 in the mouse results in distal renal tubular acidosis and decreased gastric acid secretion. Deletion of Slc26a7 decreased basolateral Cl^-/HCO_3^- exchanger activity in the acid-secreting cells in OMCD and resulted in renal bicarbonate wasting with subsequent metabolic acidosis. In the stomach, deletion of Slc26a7 reduced gastric acid secretion either due to impaired ability to extrude bicarbonate across the basolateral membrane or secondary to reduced chloride entry in the parietal cell.

The schematic diagrams in Fig. 6 depict the role of Slc26a7 in acid secretion in the kidney outer medullary collecting duct and stomach. In the kidney (Fig. 6*A*), Slc26a7 functions predominantly as a Cl^-/HCO_3^- exchanger that is active in hypertonic milieu. AE1, on the other hand, is a Cl^-/HCO_3^- exchanger that is predominantly functional in isotonic or hypotonic environment. The expression of AE1 in OMCD increased in Slc26a7 ko mice (supplemental material). Whether this adaptation is secondary to acidosis or indicates a closer interaction between Slc26a7 and AE1 remains to be determined.

Whether the role of Slc26a7 in acid secretion in the stomach is via increased bicarbonate extrusion across the basolateral membrane or enhanced entry of chloride in parietal cells via chloride conductance (Fig. 6*B*, *left* and *right panels*) remains speculative at the present. The expression of AE2 remained unchanged in gastric parietal cells in Slc26a7. Whether AE2 and Slc26a7 show differential regulation under different signaling pathways remains speculative at the present. We propose that SLC26A7 dysfunction should be investigated as a potential cause of unexplained distal renal tubular acidosis or decreased acid secretion in the stomach in humans.

REFERENCES

1. Alper, S. L., Natale, J., Gluck, S., Lodish, H. F., and Brown, D. (1989) *Proc. Natl. Acad. Sci. U.S.A.* **86,** 5429–5433
2. Schuster, V. L. (1993) *Annu. Rev. Physiol.* **55,** 267–288
3. Weiner, I. D., Wingo, C. S., and Hamm, L. L. (1993) *Am. J. Physiol.* **265,** F406–F415
4. Karet, F. E. (2002) *J. Am. Soc. Nephrol.* **13,** 2178–2184
5. Rabon, E., Cuppoletti, J., Malinowska, D., Smolka, A., Helander, H. F., Mendlein, J., and Sachs, G. (1983) *J Exp. Biol.* **106,** 119–133
6. Campbell, V. W., and Yamada, T. (1989) *J. Biol. Chem.* **264,** 11381–11386
7. Forte, J. G., and Machen, T. E. (1975) *J Physiol.* **244,** 33–51
8. Berglindh, T. (1977) *Gastroenterology* **73,** 874–880
9. Muallem, S., Burnham, C., Blissard, D., Berglindh, T., and Sachs, G. (1985) *J. Biol. Chem.* **260,** 6641–6653
10. Xu, J., Song, P., Miller, M. L., Borgese, F., Barone, S., Riederer, B., Wang, Z., Alper, S. L., Forte, J. G., Shull, G. E., Ehrenfeld, J., Seidler, U., and Soleimani, M. (2008) *Proc. Natl. Acad. Sci. U.S.A.* **105,** 17955–17960
11. Stuart-Tilley, A., Sardet, C., Pouyssegur, J., Schwartz, M. A., Brown, D., and Alper, S. L. (1994) *Am. J. Physiol.* **266,** C559–C568
12. McDaniel, N., Pace, A. J., Spiegel, S., Engelhardt, R., Koller, B. H., Seidler, U., and Lytle, C. (2005) *Am. J. Physiol. Gastrointest. Liver Physiol.* **289,** G550–G560
13. Gawenis, L. R., Ledoussal, C., Judd, L. M., Prasad, V., Alper, S.L., Stuart-Tilley, A., Woo, A. L., Grisham, C., Sanford, L. P., Doetschman, T., Miller, M. L., and Shull, G. E. (2004) *J. Biol. Chem.* **279,** 30531–30539
14. Recalde, S., Muruzábal, F., Looije, N., Kunne, C., Burrell, M. A., Sáez, E., Martínez-Ansó, E., Salas, J. T., Mardones, P., Prieto, J., Medina, J. F., and Elferink, R. P. (2006) *Am. J. Pathol.* **169,** 165–176
15. Bissig, M., Hagenbuch, B., Stieger, B., Koller, T., and Meier, P. J. (1994) *J. Biol. Chem.* **269,** 3017–3021
16. Hästbacka, J., de la Chapelle, A., Mahtani, M. M., Clines, G., Reeve-Daly, M. P., Daly, M., Hamilton, B. A., Kusumi, K., Trivedi, B., and Weaver, A. (1994) *Cell* **78,** 1073–1087
17. Schweinfest, C. W., Henderson, K. W., Suster, S., Kondoh, N., and Papas, T. S. (1993) *Proc. Natl. Acad. Sci. U.S.A.* **90,** 4166–4170
18. Everett, L. A., Glaser, B., Beck, J .C., Idol, J. R., Buchs, A., Heyman, M., Adawi, F., Hazani, E., Nassir, E., Baxevanis, A. D., Sheffield, V. C., and Green, E. D. (1997) *Nat. Genet.* **17,** 411–422
19. Zheng, J., Shen, W., He, D. Z., Long, K. B., Madison, L. D., and Dallos, P. (2000) *Nature* **405,** 149–155
20. Lohi, H., Kujala, M., Kerkelä, E., Saarialho-Kere, U., Kestilä, M., and Kere, J. (2000) *Genomics* **70,** 102–112
21. Lohi, H., Kujala, M., Makela, S., Lehtonen, E., Kestila, M., Saarialho-Kere, U., Markovich, D., and Kere, J. (2002) *J. Biol. Chem.* **277,** 14246–14254
22. Vincourt, J. B., Jullien, D., Amalric, F., and Girard, J. P. (2003) *FASEB J.* **17,** 890–892
23. Mount, D. B., and Romero, M. F. (2004) *Pflugers Arch* **447,** 710–721
24. Soleimani, M. (2006) *Novartis Found. Symp.* **273,** 91–102
25. Melvin, J. E., Park, K., Richardson, L., Schultheis, P. J., and Shull, G. E.

(1999) *J. Biol. Chem.* **274,** 22855–22861
26. Soleimani, M., Greeley, T., Petrovic, S., Wang, Z., Amlal, H., Kopp, P., and Burnham, C. E. (2001) *Am. J. Physiol. Renal Physiol.* **280,** F356–F364
27. Wang, Z., Petrovic, S., Mann, E., and Soleimani, M. (2002) *Am. J. Physiol. Gastrointest. Liver Physiol.* **282,** G573–G579
28. Petrovic, S., Ju, X., Barone, S., Seidler, U., Alper, S. L., Lohi, H., Kere, J., and Soleimani, M. (2003) *Am. J. Physiol. Gastrointest. Liver Physiol.* **284,** G1093–G1103
29. Petrovic, S., Barone, S., Xu, J., Conforti, L., Ma, L., Kujala, M., Kere, J., and Soleimani, M. (2004) *Am. J. Physiol. Renal Physiol* **286,** F161–F169
30. Xu, J., Henriksnas, J., Barone, S., Witte, D., Shull, G. E., Forte, J. G., Holm, L., and Soleimani, M. (2005) *Am. J. Physiol. Cell Physiol.* **289,** C493–C505
31. Schweinfest, C. W., Spyropoulos, D. D., Henderson, K. W., Kim, J.H., Chapman, J. M., Barone, S., Worrell, R. T., Wang, Z., and Soleimani, M. (2006) *J. Biol. Chem.* **281,** 37962–37971
32. Kim, K. H., Shcheynikov, N., Wang, Y., and Muallem, S. (2005) *J. Biol. Chem.* **280,** 6463–6470
33. Dorwart, M. R., Shcheynikov, N., Wang, Y., Stippec, S., and Muallem, S. (2007) *J. Physiol.* **584**, 333–345
34. Romero, M. F., Chang, M. H., Plata, C., Zandi-Nejad, K., Mercado, A., Broumand, V., Sussman, C. R., and Mount, D. B. (2006) *Novartis Found Symp* **273,** 126–138
35. Barone, S., Amlal, H., Xu, J., Kujala, M., Kere, J., Petrovic, S., and Soleimani, M. (2004) *J. Am. Soc. Nephrol.* **15,** 2002–2011
36. Xu, J., Worrell, R. T., Li, H. C., Barone, S. L., Petrovic, S., Amlal, H., and Soleimani, M. (2006) *J. Am. Soc. Nephrol.* **17,** 956–967
37. Schuster, V. L., Fejes-Tóth, G., Naray-Fejes-Tóth, A., and Gluck, S. (1991) *Am. J. Physiol.* **260**, F506–F517
38. Schwartz, G. J., Satlin, L. M., and Bergmann, J. E. (1988) *Am. J. Physiol.* **255**, F1003–F1014
39. Silver, R. B., and Soleimani, M. (1999) *Am. J. Physiol.* **276**, F799–F811
40. Hassoun, H., Wang, Y., Vassiliadis, J., Lutchman, M., Palek, J., Aish, L., Aish, I. S., Liu, S. C., and Chishti, A. H. (1998) *Blood* **92,** 1785–1792
41. Stehberger, P. A., Shmukler, B. E., Stuart-Tilley, A. K., Peters, L. L., Alper, S. L., and Wagner, C. A. (2007) *J. Am. Soc. Nephrol.* **18,** 1408–1418
42. Petrovic, S., Wang, Z., Ma, L., and Soleimani, M. (2003) *Am. J. Physiol. Renal Physiol.* **284,** F103–F112